International Journal of Wildland Fire
doi: 10.1071/WF20140_AC

Supplementary material

An evaluation of empirical and statistically-based smoke plume injection height parametrizations used within air quality models

Joseph L. Wilkins[A,B,C,G], George Pouliot[A], Thomas Pierce[A], Amber Soja[D,E], Hyundeok Choi[D,E], Emily Gargulinski[D], Robert Gilliam[A], Jeffrey Vukovich[F] and Matthew S. Landis[A]

[A]Office of Research and Development, US Environmental Protection Agency, Research Triangle Park, NC 27709, USA.

[B]School of Environmental and Forest Sciences, University of Washington, Seattle, WA 98195, USA.

[C]Interdisciplinary Studies Department, Howard University, Washington, DC 20059, USA.

[D]National Institute of Aerospace, Hampton, VA 23666, USA.

[E]NASA Langley Research Center, Hampton, VA 23666, USA.

[F]Office of Air and Radiation, US Environmental Protection Agency, Research Triangle Park, NC 27709, USA.

[G]Corresponding author. Email: joseph.wilkins@howard.edu

S1. CALIOP-derived retrievals

This supplemental section provides additional references and discussions related to the CALIOP-derived retrieval methodology for data extraction and filtering. This method is described in detail in Soja *et al.* (2012); a summary is provided here for the CALIOP back trajectories. For the 2013 California Rim Fire, satellite imagery was used to estimate plume height tops. We used the Cloud-Aerosol Lidar with Orthogonal Polarization (CALIOP) instrument on board the Cloud-Aerosol Lidar and Infrared Pathfinder Satellite Observations (CALIPSO) satellite to map the vertical distribution of atmospheric aerosols and clouds (Omar *et al.* 2009, http://www-calipso.larc.nasa.gov/). A plume injection height product was built by extracting smoke-plume aerosols "curtains" (indicating width and frequency) from CALIOP's tracks (Fig. S1), with data resolved at 100-m vertical and 1-s horizontal intervals.

CALIOP tracks (Fig. S2) were overlaid on NOAA's Hazard Mapping System (HMS) smoke product. CALIPSO aerosol data were then extracted and used to initialize the Langley Trajectory Model (LaTM). We used NASA's Modern-Era Retrospective Analysis for Research and Application version 2 (MERRA2) assimilated meteorological data to drive the simulations (Gelaro *et al.* 2017). This fire-smoke plume was further verified using visible satellite imagery compared to the overlaid CALIPSO tracks. The LaTM initialized with the CALIOP observations was driven by NASA Goddard Earth Observing System version 5 (GEOS-5) large-scale meteorological reanalysis data (Molod *et al.* 2015). Fire-smoke trajectories were computed backwards in three-dimensional space and time (15-min time steps) until horizontally coincident (~20 km) with daily Moderate Resolution Imaging Spectroradiometer (MODIS) fire detections (Giglio *et al.* 2003; Pierce *et al.* 2003, 2009). Trajectories were initialized at ~1-s intervals along

the CALIPSO-derived smoke segment track within the fire-smoke plume and at 100-m vertical intervals.

As fire-smoke trajectories are traced back in time, several unique coincidences with fires on-ground can be used to determine daily smoke plume injection height and detrainment (Soja *et al.* 2012). Uncertainties with this method are primarily due to satellite limitations with detection of fire-smoke elevation, smoke source attribution, and fire locations. MODIS fire detection positions are generally accurate. Therefore, CALIPSO's narrow swath width must coincide with the smoke plume extent (Fig. 4). CALIOP is able to detect optically thin smoke layers at a fine vertical resolution, but the smoke must be in the same direction of the overpass.

Moreover, the modeled plume top using GEOS-5 is defined by a threshold, where the plume top height is equal to the height where modeled carbon monoxide from a wildfire first exceeds 20 ppb from model top going to the surface (Soja *et al.* 2012). However, based on CALIPSO tracks, for certain days and fires, data may not be available if the tracks do not cross smoke plumes. These data gaps are filled in using the GEOS-5 model; therefore, uncertainties are inherent within the model predictions, because they rely on plume height inputs several kilometers downwind in addition to the dependence on meteorological inputs. The values used in this study are the shaded range between the mean and maximum values per hour from these trajectories. Figure S3 depicts the mean values and Figure S4 the minimum values of the smoke plume tops from the method described above.

S2. Operational details for the CL-51 and MiniMPL

This section summarizes the operational details for the Ceilometer CL51 (CL-51) and the Hexagon Miniaturized Micro Pulse LiDAR (MiniMPL). For the prescribed burns at the Konza

Prairie Biological Research Station, we used two lidar instruments to measure plume heights (MiniMPL) and boundary layer heights (CL-51). A MiniMPL (Spinhirne 1993; Spinhirne *et al.* 1995a,b) uses a pulse energy of 3-4 μJ at 2500 Hz to measure backscatter intensity with an eye-safe (ANSI Class II) laser at a wavelength 0.53 μm. The customized MiniMPL system is equipped with an automated scanning apparatus with a range of 360˚ azimuth and 0-90˚ elevation, a rifle scope, and a GoPro camera. The MiniMPL provides near-range atmospheric lidar retrievals acquired up to a range of 15 km at a user-selected grid spacing of 5/15/30/75 m, with accumulation time of 1 s-15 min (Welton and Campbell 2002). Operational details are summarized in Table S1. We used the scanning MiniMPL during each experimental burn to measure the characteristics of the smoke plume (Fig. S5). A combination of plan position indicator (PPI) and range height indicator (RHI) scans was used to collect radial velocities and aerosol backscatter data across predetermined horizontal sectors covering the burn plots (Kovalev *et al.* 2005; Charland and Clements 2013). An example scanning scenario is as follows:

i. A RHI or PPI scan is taken, likely using a scanning scenario or pattern, generating a pulse at the elevation angle (***θ***) and azimuths angles *(ϕ)* in degrees.

ii. The lidar signal continues until it is attenuated at a given distance (usually identified by the signal-to-noise ratio reaching its peak, near or more than 1).

iii. The distance to attenuation is recorded when the pulse returns to the lidar (***ε)*** in meters.

iv. Assuming that the lidar relative to the field creates a right angle, we can calculate the height relative to the lidar as [***Sin (θ) = opp/Hyp***] or { $\alpha = \text{Sin}(\theta) * \varepsilon$ }.

v. With, α, the relative height above the lidar, we add the height above the lidar (**β**), either in height above sea level (asl) or height above the geoid, or terrain.

vi. $H_{PLUMETOP} = \alpha + \beta$ (ASL or geoid or terrain); values in this study are reported as ASL. For example;

***PBL = 854 m , ε = 1560 m, θ = 15˚ (elevation angle), (ϕ) = 260˚ (azimuth angle),* β = *404 m (above sea level) or 60 m (above terrain),* α = Sin (*15*) * *1560* m = 403 m | $H_{PLUMETOP}$ = 403 + 404 = 807 m**

The thickness of the plume is determined by the signal-to-noise ratio. For Konza Prairie Burn 3, the lidar performed RHI and PPI sector scan patterns between 260˚ and 275˚ azimuths at an elevation angle of -9˚ to 9˚, stepping by 3˚ at the location indicated in Figure 1 for 16 March 2017. For Burn 4, the lidar performed RHI and PPI sector scan pattern between 340˚ and 300˚ azimuths at an elevation angle of 0˚ to 20˚, stepping by 2˚ at the location indicated in Figure 1 for 16 March. Retrievals for Burns 3 and 4 are shown in Figure 6. Retrievals for Burn 5 (20 March; Fig. S5) were a bit more complicated due to the varying winds and width of fields burned in close proximity with similar starting times.

Two Vaisala Model CL-51 ceilometers (Münkel *et al.* 2007) were deployed during the Konza Prairie prescribed burn to estimate the PBL height (McKendry *et al.* 2009, 2010; Tsaknakis *et al.* 2011; Liu *et al.* 2012; Clements and Oliphant 2014). The CL-51 emits short, powerful laser pulses in a stationary vertical direction and operates at a wavelength of 0.9 μm. This wavelength is sensitive to the fine particulate matter ($PM_{2.5}$) found in smoke plumes. Using the Vaisala BL-View software, PBL heights were collected and stored at a vertical grid spacing of 20 m with a 2-s detection frequency (Fig. S6).

S3. Planetary Boundary Layer (PBL) analysis

To gauge the efficacy of a plume rise algorithm, we compared the modeled and observationally derived PBL bias information for each burn (Konza Prairie: Fig. S6; Rim Fire and Konza: Fig. S7). Figure S7 shows the time series comparison of the PBL diurnal profile during each burn (Konza burns: Fig. S7a; Rim Fire burns: Fig. S7c). A comparison of the observations to model stable layers showed that the model performed better for the Konza prescribed grassland burns [mean bias (MB) ±400 m) than for the Rim wildfire (MB +1000 m)]. Further, as expected, the PBL was better constrained in the 4-km simulation than in the 12-km simulation; in the 4-km simulation, bias switched from negative to positive, and error lowered (~5 m). A comparison of the modeled PBL to observations from the ground-based CL-51 (Figs. S6, S7b) and the satellite-based CALIOP (Fig. S7d) demonstrates that the diurnal evolution of the PBL was better captured for the Rim Fire burns (R^2=0.5) than for the Konza Prairie burns (R^2=0.1). There appeared to be a very weak nighttime connection between the CL-51-measured PBL and CMAQ-modeled PBL, with a lag in the PBL growth 1 to 3 hours in the model. The model lag is likely due to the difference between a 4- to 12-km grid averaged PBL height versus a single-point CL-51 measurement location. The range of overall error between the modeled and measured PBL height was 5-40 m.

S4. SMOKE model details

Model plume heights were evaluated for the plume rise algorithms in the Sparse Matrix Operator Kernel Emissions (SMOKE; https://www.cmascenter.org/smoke/) modeling system (Coats Jr. *et al.* 1997), which is used in the Community Multiscale Air Quality (CMAQ) modeling system. SMOKE was initialized with fire data extracted from BlueSky Framework

using SMARTFIRE2 (Raffuse *et al.* 2009, 2012); the meteorological option is outlined in Table S1. Figure S8 depicts the WRF model domain (see S5, Weather and Research Forecasting (WRF) Model (WRF 12km and 4km).

SMOKE uses spatial allocation (horizontal and vertical), temporal allocation, and chemical speciation algorithms that process emissions into a form that can be ingested by an AQM. Thus, chemically-speciated emissions for each wildland fire are distributed hourly to the appropriate three-dimensional grid cells. SMOKE models the time of burn based on a temporal profile for fires (see SMOKE 4.0 Manual Section 4.4.17, Plume Rise Calculation for Fires). The SMARTFIRE2 inventory was used to reconcile the sources of fire activity data (Sullivan *et al.* 2008). The process of reconciling fires from incident status summary report (ICS-209) with SMARTFIRE2 is described by Raffuse *et al.* (2007, 2012). Wildland fire emission inventories have been estimated each year since 2002 (ftp://ftp.epa.gov/EmisInventory/fires, accessed 16 October 2017). After the fire reconciliation process was completed, for the Rim Fire, the biomass fuel consumption was calculated using the U.S. Forest Service's CONSUME 3.0 fuel consumption model (https://www.fs.fed.us/pnw/fera/fft/consumemodule.shtml, accessed 16 October 2017) and the Fuel Characteristic Classification System (FCCS) fuel-loading database in the BlueSky Framework (Ottmar *et al.* 2007). Emission factors were taken from the Fire Emission Production Simulator (FEPS) model (https://www.fs.fed.us/pnw/fera/feps, accessed 16 October 2017). For the Konza Prairie prescribed burns (March 2017), Table 1 shows the field data used to support the model.

In this analysis, we compared the SMOKE model, using different vertical allocation (or plume rise) methods, against observations from the wildfire (Rim Fire: CALIOP observations) and the prescribed burn (Konza Prairie: MiniMPL observations). Plume rise in SMOKE

(controlled by the LAYPOINT code) can be precomputed externally or computed internally. In this study, smoke-plume heights were calculated internally (Table 2: formulations; Table 3: details and full model formulation details for each plume rise algorithm). SMOKE's internal calculation of plume rise (referred to hereafter as BASELINE) uses the Briggs plume rise formulation (Pouliot *et al.* 2005), size of area burned, and fuel loading, and adjusts for time of burn using a temporal profile for fires (SMOKE 4.0 Manual Section 4.4.17, Plume Rise Calculation for Fires). In summary, this process requires two separate input inventory files: (i) a list of fire-specific characteristics, including county/state/country, fire identification, location coordinate, fire name, source classification codes and others (SMOKE 4.0 Manual, Section 8.2.8.3), and (ii) day-specific fire data, including size of area burned, fuel loading, and start/end hour of fire (SMOKE 4.0 Manual, Section 8.2.6.2).

S5. Weather and Research Forecasting (WRF) Model (WRF 12km and 4km).

Figure S8 shows a map of the two nested Weather and Research Forecasting (WRF) domains, at 12-km and 4-km horizontal resolution, both with 40 vertical levels. Table S2 shows the model configuration; the model was run with two-way nesting, using the Pliem-Xiu boundary layer scheme (Xiu and Pliem, 2001), the Kaine-Fritsch convective parameterization (Kain, 2004), and the NOAH land surface scheme (Ek, 2003). WRF v3.8.1 nested 12- and 4-km simulations using the standard U.S. EPA WRF configuration with Four-Dimensional Data Assimilation (FDDA) on the 12 km domain and no FDDA on nested domains. The WRF model was spun up from 1 to 9 March 2017 for the evaluation focus period of 10-31 March 2017.

Figure S9 shows RMSE of WRF-simulated tropospheric temperature at the Topeka, Kansas, rawinsonde sounding site for 10-31 March 2017 for the 12- and 4-km simulations. Very little difference was found between the meteorological data inputs. The figure shows the consistency

at the surface and aloft across the different modeling domains for the given study area.

S6. Sofiev algorithm explanation

The first alternative plume rise algorithm was an empirical, energy-balance-based parameterization (similar to convective cloud formulations) designed for fires (Sofiev *et al.* 2012) and was implemented at 12- and 4-km grids (hereafter SOFIEV12KMHR and SOFIEV4KMHR). Table S3 lists all the energy balance general equations. Briefly, the equation accounts for meteorological parameters and fire intensity. The meteorological parameters are the reference and the free troposphere (FT) Brunt-Väisälä frequency ($N_0^2 = 2.5 \text{ x } 10^{-4}\text{s}^{-2}$; N_{FT}^2) and the height of PBL (H_{PBL}). Fire intensity consists of the reference FRP ($P_{f0} = 10^6$ W) and the observed or calculated FRP (FRP_{calc}). The equation has four fitted, tunable calibration constants: α, β, γ, and δ, which were originally tested and set to match observed plume heights by MISR. α is the part of the plume that passed the PBL freely; β is the weighted contribution of the fire intensity; γ is the determined power-law dependence on FRP (injection height will be proportional to FRP to the power of 0.5, because this ratio provides the plume height upper limit without losses to friction and changing atmospheric and plume parameters); and δ defines the plume atmospheric stability dependence in the FT. Where measured FRP was not available, it was derived (FRP_{calc} = heat flux * 0.1 * area burned), using the model heat flux and area burned, assuming that radiative energy was 10% of the total fire heat energy (Wooster *et al.* 2005; Val Martin *et al.* 2012).

References for Supplemental Materials

Ek MB, Mitchell KE, Lin Y, Rogers E, Grunmann P, Koren V, Gayno G, Tarpley JD (2003) Implementation of Noah land surface model advances in the National Centers for Environmental Prediction operational mesoscale Eta model. Journal of Geophysical Research-Atmopsheres 108(D22), 8851, https://doi.org/10.1029/2002JD003296.

Kain JS (2004) The Kain-Fritsch Convective Parameterization: An Update. Journal of Applied Meteorology 43(1), 170-181, https://doi.org/10.1175/1520-0450(2004)043<0170:TKCPAU>2.0.CO;2.

Iacono MJ, Delamere JS, Mlawer EJ, Shephard MW, Clough SA, Collins WD (2008) Radiative forcing by long-lived greenhouse gases: calculations with the AER radiative transfer models. Journal of Geophysical Research 113, D13103, doi:10.1029/2008 JD009944.

Pleim JE (2007a). A combined local and non-local closure model for the atmospheric boundary layer. Part 1: Model description and testing. Journal of Applied Meteorology Climatology 46, 1383–1395.

Pleim JE (2007b). A combined local and non-local closure model for the atmospheric boundary layer. Part 2: Application and Evaluation in a Mesoscale Meteorological Model. Journal of Applied Meteorology Climatology 46, 1396–1409.

Skamarock WC, Klemp JB, Dudhia J, Gill DO, Barker DM, Duda MG, Huang XY, Wang W, Powers JG (2008) A description of the advanced research WRF Version 3. NCAR Technical Note, NCAR/TN-475+STR. Mesoscale and Microscale Meteorology Division, National Center for Atmospheric Research, Boulder, CO, USA.

Xiu A, Pleim JE (2001) Development of a land surface model. Part I: application in a mesoscale meteorological model. Journal of Applied Meteorology 40, 192-209.

Supplemental Materials: Figures and Tables

Table S1. MiniMPL and Ceilometer (CL-51) information.

	Hexagon **MiniMPL**	**Vaisala** **CL-51**
Range resolution	User selectable 5/15/30/75 m	10 m
Minimum range	100 m	5 m
Accumulation time	1 sec – 15 min	6-160 s
Detection range	Up to 18 km	Up to 15 km
Scanning	Yes	Vertical or 12˚ titled
Laser wavelength	532 nm	910 nm
Laser pulse frequency	2500 Hz	6500 Hz
Detector	Fiber coupled	InGaAs diode
Size (mm)	380 x 305 x 480	834 x 266 x 264
Weight	13 kg	18.6 kg
Power requirement	100 W	310 W

Table S2. Model configurations.

		Options	**References**
Meteorology Options	Off-line	Yes	
	WRF version 3.8.1		Skamarock et al, 2008
	Initialization	NCEP/NCAR Reanalysis	Skamarock et al, 2008
	FDDA	NCEP/NCAR Reanalysis	Skamarock et al, 2008
	Landuse	MODIS	
	Cumulus Parameterization	Kain–Fritsch 2 cumulus parameterization	Kain, 2004
	Radiation	RRTMg	Iacono *et al.* 2008
	PBL	Asymmetric Convective Model version 2	Pleim, 2007a and b
	Land Surface Model	Pleim-Xu	Xiu and Pleim, 2001

Table S3. Plume rise model configurations.

	Smoke-Briggs	**Sofiev 2012**	**Pbl + 500m**
Formulation	$H_{top} = \begin{cases} 1.2\left[\left(\frac{F}{W*U^2}\right)^{0.6} * \left(1.3\frac{F}{W*U^2}\right)^{0.4}\right] & neutral \\ 2.6\left(\frac{F}{W*S}\right)^{1/3} & stable \\ 30.0\left(\frac{F}{W}\right)^{0.6} & unstable \end{cases}$ $H_{bottom} = \frac{2}{3}\left(\frac{H_{top}}{2}\right)$ Q = AB * FL * HC * 2000 / DT $F = Q \times 2.58 \times 10^{-6}$ $E = 0.0703 \times \ln(A) + 0.3$ $S_{fract} = 1 - BE_{size}$ $s = g\,\frac{\frac{\partial\theta}{\partial z}}{\theta}$ H_{top}, H_{bottom}: plume top and bottom Q: heat flux (BTU/hr) AB: area burned (acre/day) FL: Fuel Loading (tons/acre) HC: Heat Content (BTU/lb) DT: Duration of fire (hr/day) F: Bouyancy flux (m^4/s^3) U: wind speed (m/s) BE_{size}: Buoyant efficiency S_{frac}: fraction of smoldering emissions W: Wind speed at top of stack m/s.	$H_P = \alpha H_{PBL} + \beta\left(\frac{FRP}{P_{f0}}\right)^{\gamma} \exp\left(-\delta N_{FT}^2/N_0^2\right)$ H_{PBL}: PBL height FRP: Fire radiative power P_{f0}: reference fire power, P_{f0}= 10^6 W N_0: reference Brunt-Väisälä frequency; N_0^2=2.5×10^{-4} s^{-2} N_{FT}: Brunt-Väisälä frequency α: part of PBL passed freely; $\alpha < 1$ β: weight of fire intensity contribution; $\beta > 0m$ γ: power of dependence on FRP; $\gamma < 0.5$ δ: weight of dependence on free troposphere stability; $\delta \geq 0$ Two alternative ways of setting $\alpha, \beta, \gamma, \delta$: (1) one-stage: $\alpha = 0.24;\ \beta = 170m;\ \gamma = 0.35;\ \delta = 0.6$ (2) two-stage: stage 1: $\alpha = 0.15;\ \beta = 102\,m;\ \gamma = 0.49;\ \delta = 0$ stage 2: $\alpha = 0.24;\ \beta = 170\,m;\ \gamma = 0.35;\ \delta = 0.6$ $(H_P \leq H_{pbl})$ $\alpha = 0.93;\ \beta = 298\,m;\ \gamma = 0.13;\ \delta = 0.7$ $(H_P > H_{pbl})$	H_top = PBL + 500

Comments	The main criticism of this approach is that it is based on experimental data from non-fire plumes. Buoyancy flux might not scale well from stacks to large fires. However, the performance might be improved by treating fires as multiple plumes with varied input parameters (Strand *et al.* 2007). Treatment of vertical and temporal allocation of emissions is available in SMOKE/CMAQ.	The two key parameters, FRP and N_{FT}, are not readily available from SMOKE/CMAQ but can be derived from existing variables. FRP can be derived from burned area (A) and fire heat flux (Q), which are available from BlueSky (Pouliot *et al.,* 2005), using the following equation, assuming that radiative energy is about 10% of the total fire heat energy (Wooster *et al.* 2005; Freeborn *et al.* 2008; Martin *et al.* 2012): $FRP = Q \times 0.1 \times A$ N_{FT} can be derived from potential temperature (θ): $N_{FT} = \sqrt{\frac{g}{\theta}\frac{d\theta}{dz}}$ ($z \approx 2H_{PBL}$) This approach does not provide a recipe for vertical or temporal allocation of emissions; a separate treatment is needed.	

Figure S1. CALIPSO tracks overlaid on a MODIS Visible image, showing both the vertical and horizontal extent of smoke and clouds. MODIS Terra and Aqua fire-detection data (red dots) highlight the Rim Fire burning in California on 22, 25, and 26 August 2013. The visible smoke was transported across California, Nevada, Oregon, and Idaho before intersecting with the CALIPSO track over Montana and Canada. The CALIOP smoke-aerosol vertical-profile data (black and brown) extended from the surface to ~5 km. The vertical extent and height of the clouds are evident to the south and north of the CALIOP swath, and the horizontal extent of the clouds is evident in the visible MODIS image. CALIOP data provide the vertical properties that inform the horizontal view to give a complete representation of aerosol transport and the atmosphere.

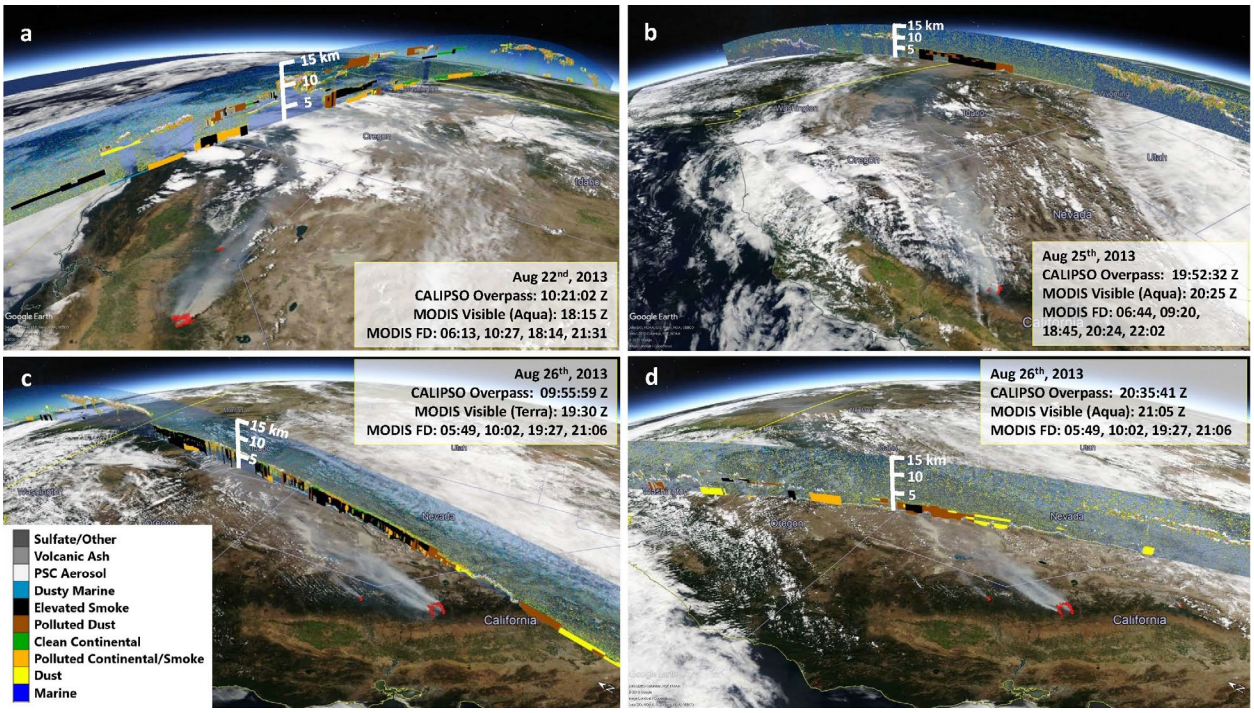

Figure S2. CALIPSO tracks used in this study; see Figure 4.

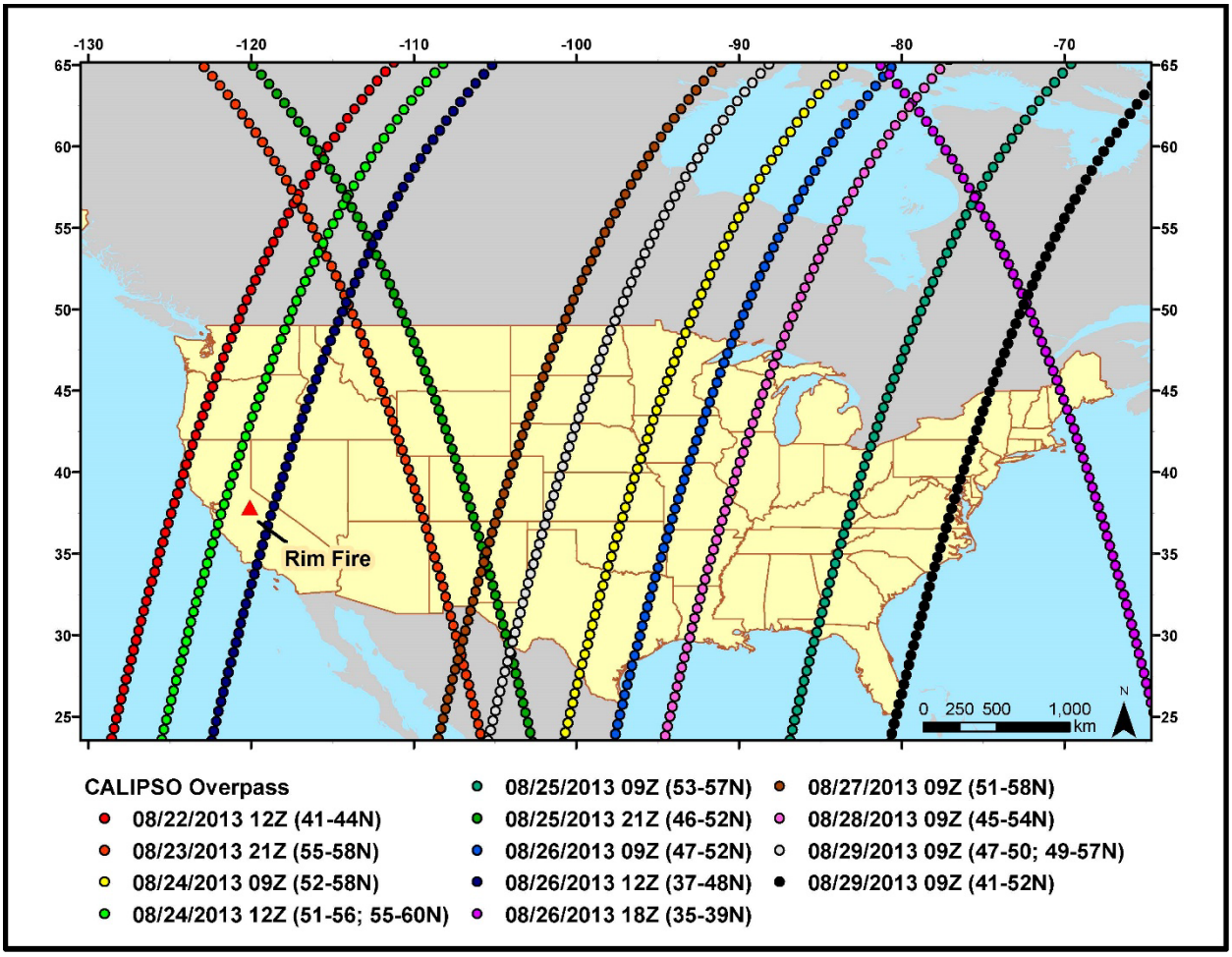

Figure S3. Mean vertical allocation of smoke-plume tops, as opposed to the maximum plume tops shown in figure 5, for the 2013 California Rim Fire (Burn 1: 21 August; Burn 2: 24 August), plotted with the planetary boundary layer (PBL) and fire radiative power (FRP). Smoke plume detrainment was derived using Cloud-Aerosol Lidar with Orthogonal Polarization (CALIOP) data. Each color represents a distinct CALIPSO overpass. For example, the 21 August smoke plume was captured by nine distinct CALIOP overpasses, and the 24 August smoke plume was captured by seven CALIOP overpasses. Each CALIOP overpass is named by the date of smoke/CALIOP data coincident, model initialized GMT time, and the location of the smoke plume in the CALIOP overpass. For example, the smoke represented in purple-blue from 21 August coincided with a CALIOP overpass on 22 August at 41-44˚ North latitude; back trajectories were initialized to connect the smoke to the fire at 12:00 UTC.

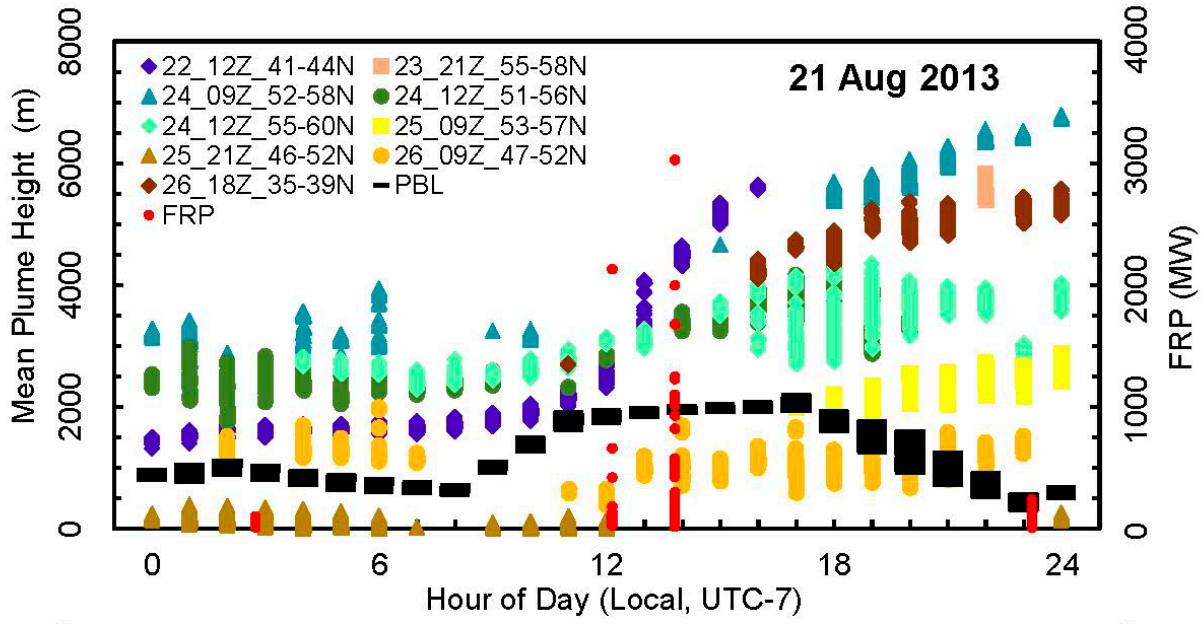
21 Aug 2013
22_12Z_41-44N
23_21Z_55-58N
24_09Z_52-58N
24_12Z_51-56N
24_12Z_55-60N
25_09Z_53-57N
25_21Z_46-52N
26_09Z_47-52N
26_18Z_35-39N
PBL
FRP
Mean Plume Height (m)
FRP (MW)
Hour of Day (Local, UTC-7)
0
2000
4000
6000
8000
1000
3000
6
12
18
24

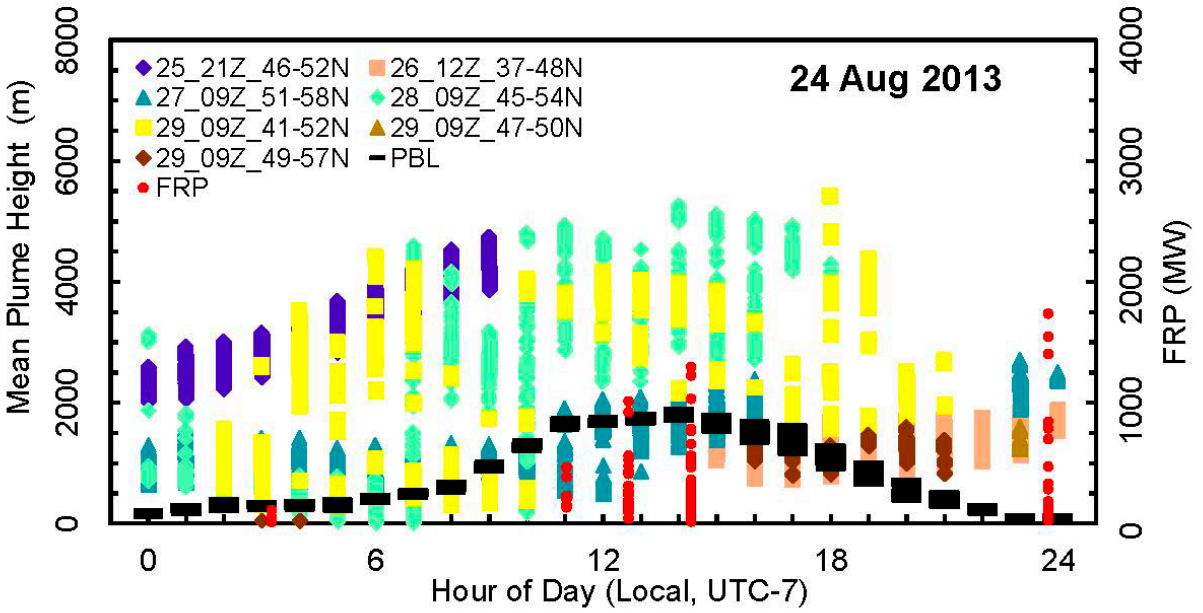
24 Aug 2013
25_21Z_46-52N
26_12Z_37-48N
27_09Z_51-58N
28_09Z_45-54N
29_09Z_41-52N
29_09Z_47-50N
29_09Z_49-57N
PBL
FRP
Mean Plume Height (m)
FRP (MW)
Hour of Day (Local, UTC-7)
0
2000
4000
6000
8000
1000
3000
6
12
18
24

Figure S4. Minimum vertical allocation of smoke-plume tops, as opposed to the maximum plume tops shown in figure 5, for the 2013 California Rim Fire (Burn 1: 21 August; Burn 2: 24 August), plotted with the planetary boundary layer (PBL) and fire radiative power (FRP). Smoke plume detrainment was derived using Cloud-Aerosol Lidar with Orthogonal Polarization (CALIOP) data. Each color represents a distinct CALIPSO overpass. For example, the 21 August smoke plume was captured by nine distinct CALIOP overpasses, and the 24 August smoke plume was captured by seven CALIOP overpasses. Each CALIOP overpass is named by the date of smoke/CALIOP data coincident, model initialized GMT time, and the location of the smoke plume in the CALIOP overpass. For example, the smoke represented in purple-blue from 21 August coincided with a CALIOP overpass on 22 August at 41-44˚ North latitude; back trajectories were initialized to connect the smoke to the fire at 12:00 UTC.

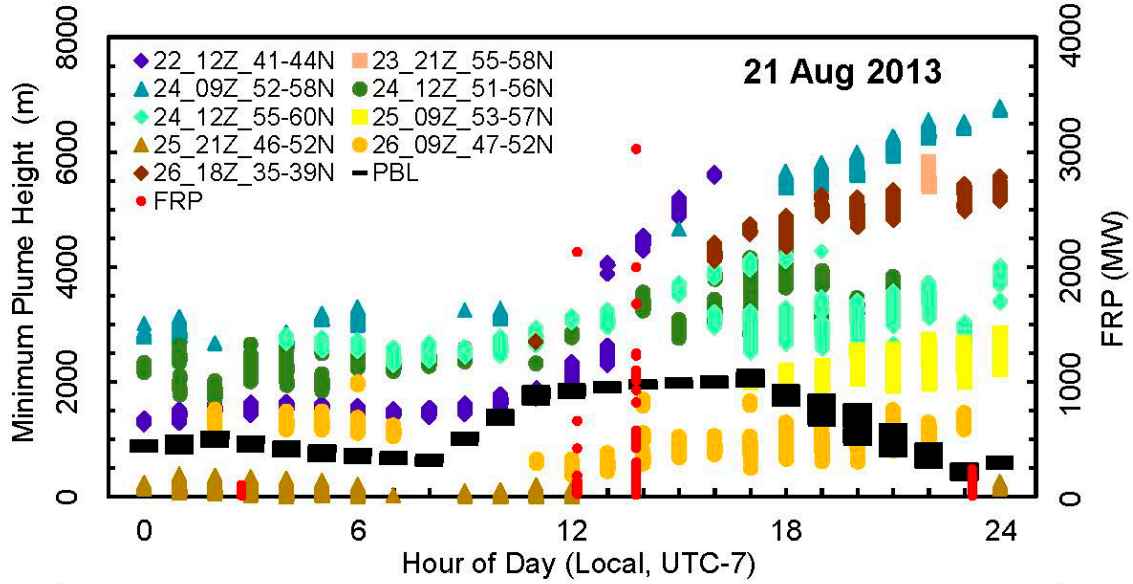
21 Aug 2013
22_12Z_41-44N
23_21Z_55-58N
24_09Z_52-58N
24_12Z_51-56N
24_12Z_55-60N
25_09Z_53-57N
25_21Z_46-52N
26_09Z_47-52N
26_18Z_35-39N
PBL
FRP
Minimum Plume Height (m)
FRP (MW)
Hour of Day (Local, UTC-7)
0
2000
4000
6000
8000
1000
3000
6
12
18
24

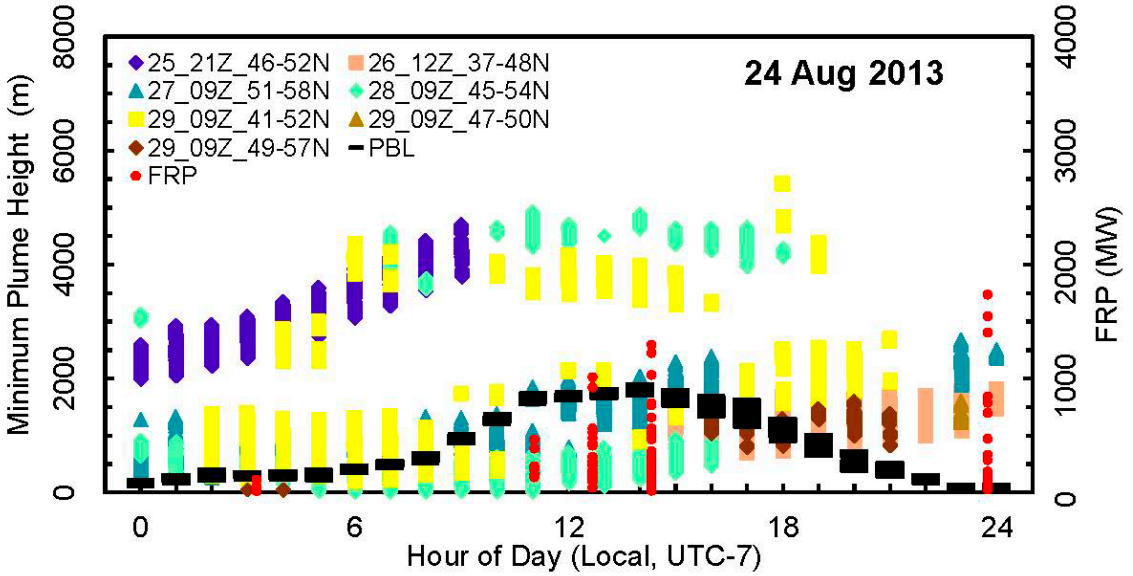
24 Aug 2013
25_21Z_46-52N
26_12Z_37-48N
27_09Z_51-58N
28_09Z_45-54N
29_09Z_41-52N
29_09Z_47-50N
29_09Z_49-57N
PBL
FRP
Minimum Plume Height (m)
FRP (MW)
Hour of Day (Local, UTC-7)
0
2000
4000
6000
8000
1000
3000
6
12
18
24

Figure S5. Prescribed burn experiment at Konza Prairie Biological Station, Kansas, in 2017 (Burn 5, 20 March 2017). Smoke-plume range height (m above sea level) and backscatter (km^2 μs^{-1} μJ^{-1}) were derived using a ground-based Hexagon Miniaturized Micro Pulse Lidar (MiniMPL). The lidar starting height was 440 m above sea level for the plume height measurements.

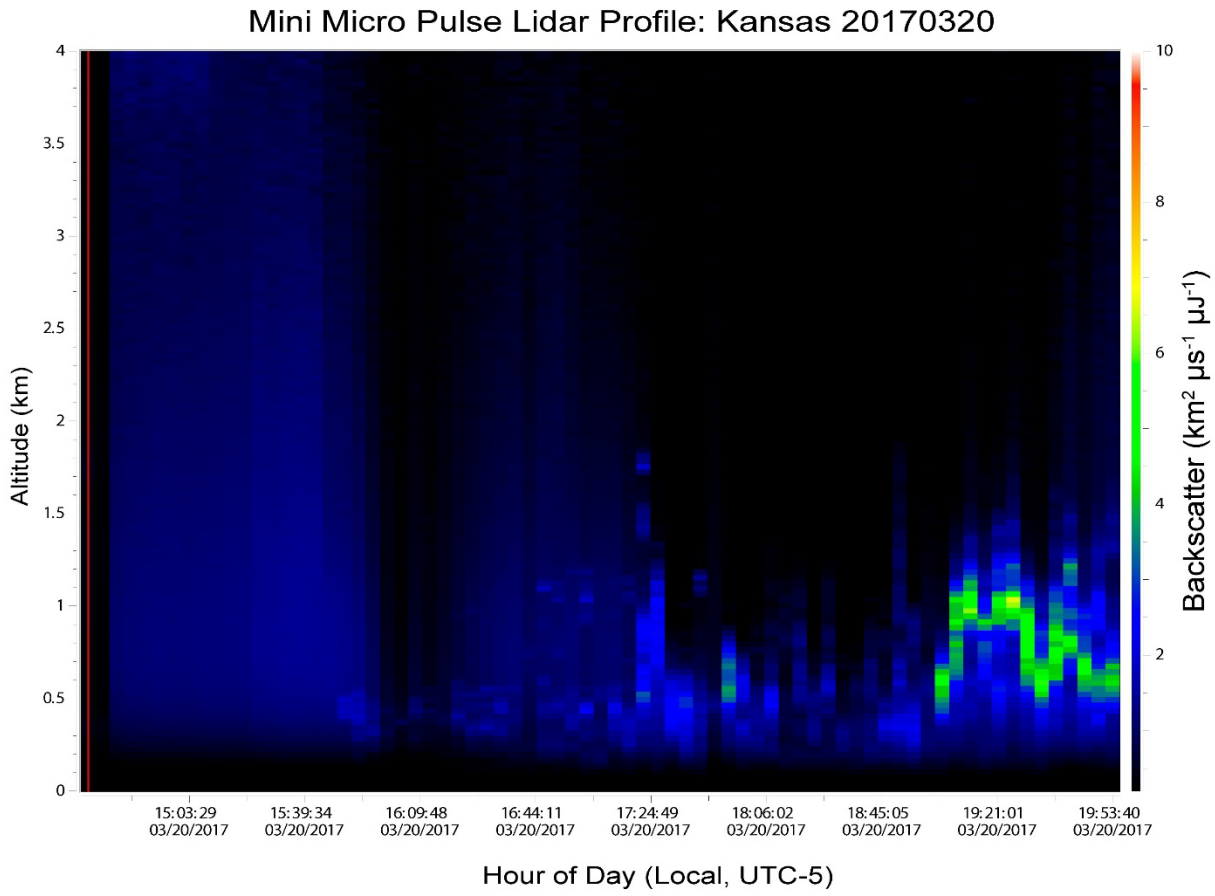

Figure S6. Prescribed burn experiment at Konza Prairie Biological Station, Kansas, in 2017. Ceilometer CL-51 raw retrievals and log backscatter for 16 March (Burns 3, 4) and 20 March (Burn 5). Black line: Planetary boundary layer height.

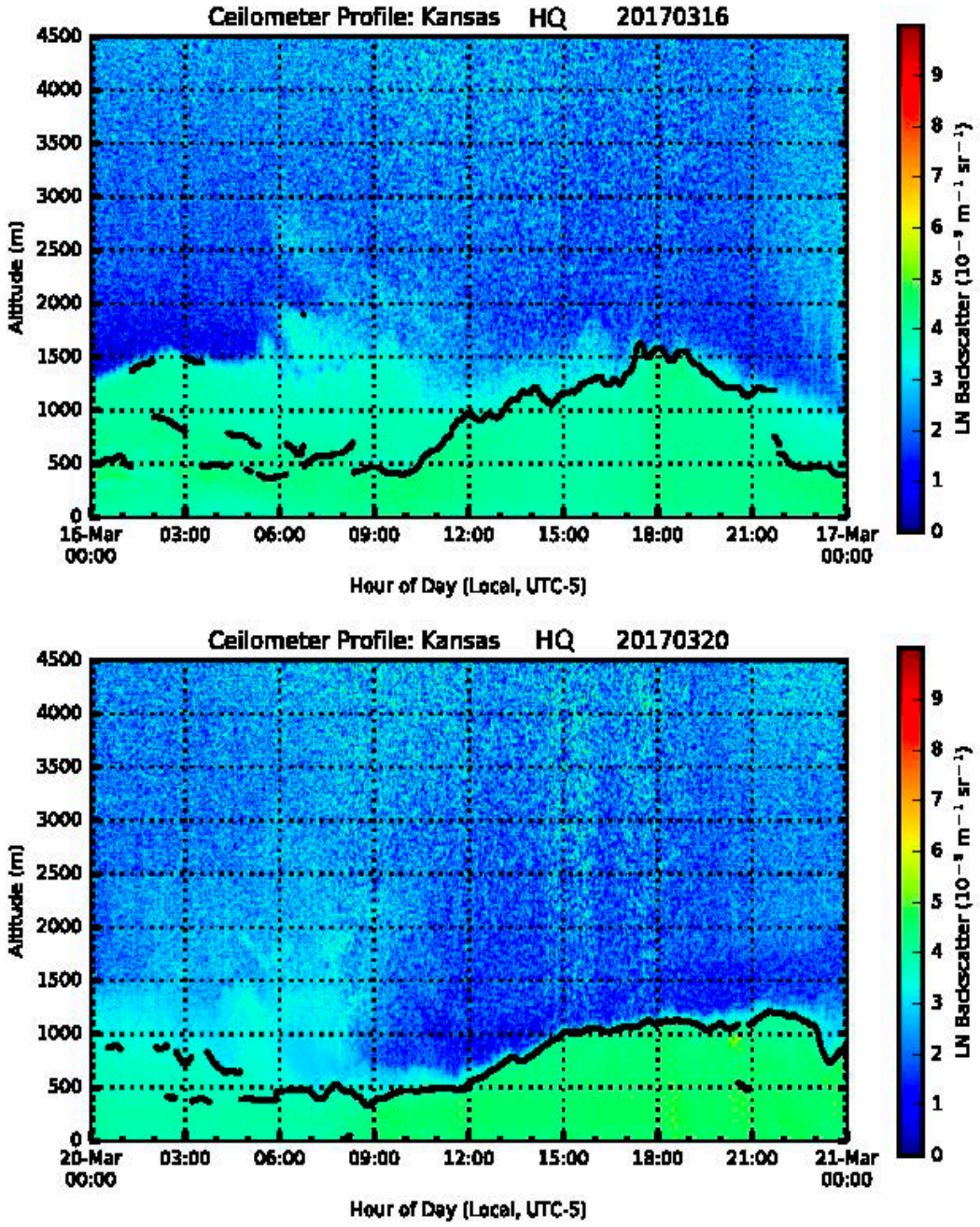

Figure S7. Comparison of observed and modeled planetary boundary layer (PBL) heights for the 2017 prescribed Konza Prairie Fire and the 2013 California Rim wildfire. (a) Konza Prairie Fire: PBL heights were derived from data taken by two Vaisala Model CL-51 ceilometers (CASNET (HQ) and NEON), and data were modeled with a 4-km and 12-km grid resolution WRF model. (b) Comparison of observed and modeled PBL heights within two hours of each Konza burn. (c) California Rim Fire: comparison of MERRA-2 and 12-km WRF (used by CMAQ) PBL heights. (d) Scatterplot of hourly data shown in the Figure 7c time series.

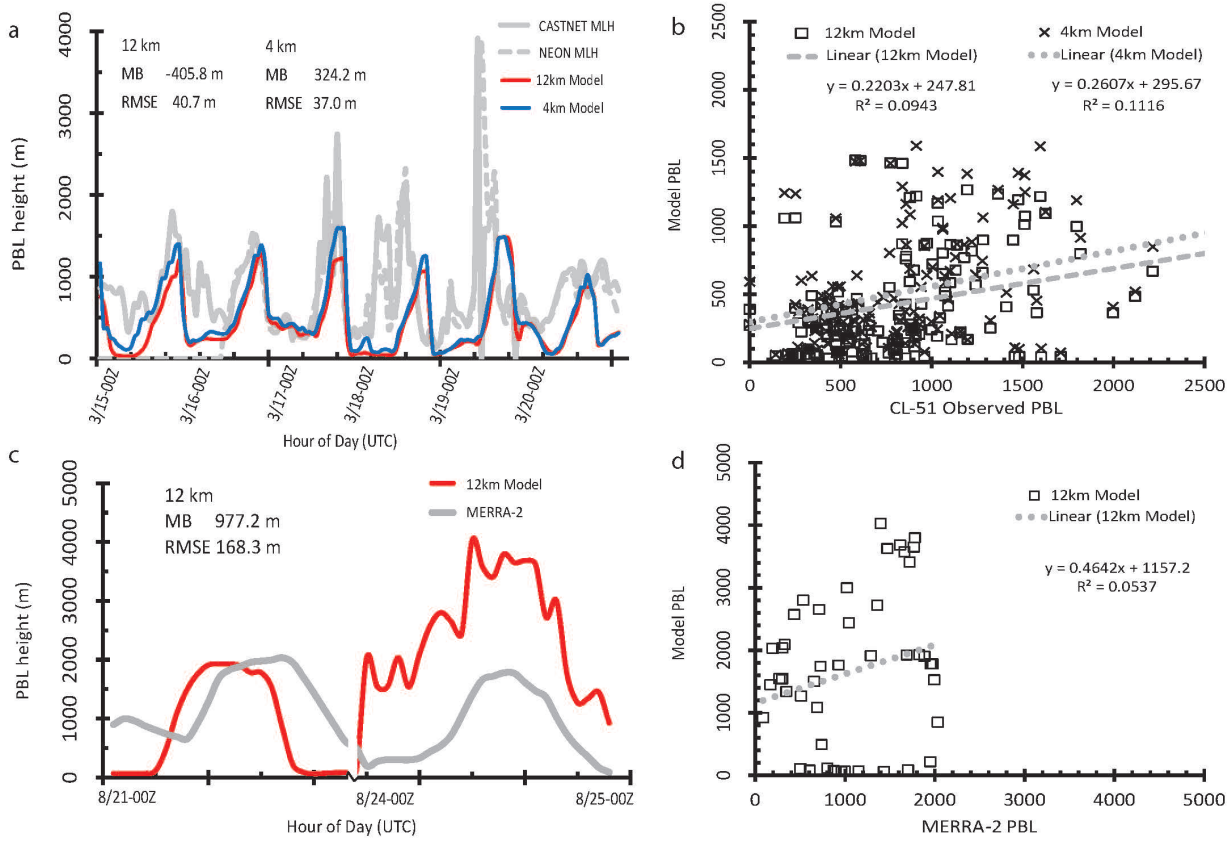

Figure S8. Two nested Weather and Research Forecasting (WRF) version 3.8.1 domains, at 12-km and 4-km horizontal resolution, both with 40 vertical levels. The 4-km domain was used exclusively for the 2017 prescribed burns at Konza Prairie, Kansas (Burns 3, 4, 5).

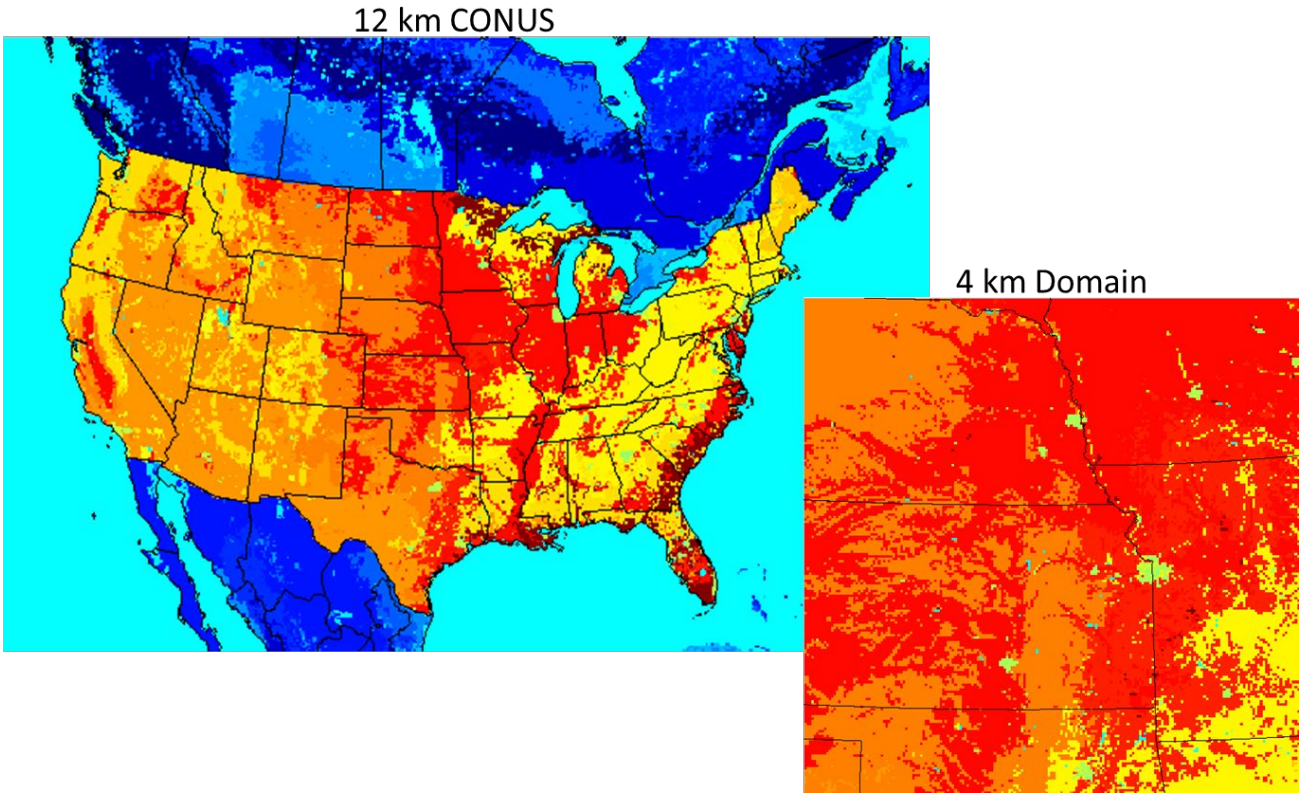

Figure S9. RMSE of WRF-simulated tropospheric temperature at Topeka, Kansas, rawinsonde sounding site for 10-31 March 2017. Left: 12-km WRF simulation; right: 4-km WRF simulation.